Materials Transactions, Vol. 58, No. 2 (2017) pp. 231 to 235

Microstructure of Erbium Oxide Thin Film on SUS316 Substrate with Y_2O_3 or CeO_2 Buffer Layers Formed by MOCVD Method

Seungwon Lee[1], Takayuki Shinkawa[2,*1], Kenji Matsuda[1,*2], Masaki Tanaka[3], Yoshimitsu Hishinuma[3], Katsuhiko Nishimura[1], Teruya Tanaka[3], Takeo Muroga[3] and Takahiro Sato[4]

[1]*Graduate School of Science and Engineering for Research, University of Toyama, Toyama 930–8555, Japan*
[2]*Graduate School of Science and Engineering for Education, University of Toyama, Toyama 930–8555, Japan*
[3]*National Institute of Fusion Science, Toki, 509–5292, Japan*
[4]*Hitachi High-Technologies Corp., Hitachinaka, 312–0057, Japan*

Er_2O_3 has been known the best candidate material for insulating coating for liquid metal breeding blanket system. The formation of Er_2O_3 layer by MOCVD method can be succeeded on SUS316 substrate with CeO_2 and Y_2O_3 buffer layers (100 nm and 500 nm) fabricated by RF sputtering, and their microstructures have been confirmed by SEM, TEM and STEM. The surface morphology of their layers was smaller granular structure than the previous study without buffer layer. According to cross sectional TEM (X-TEM) observation, Er_2O_3, CeO_2/Y_2O_3 buffer, unknown layers and SUS substrate can be confirmed. CeO_2 buffer layer has a granular structure, while Y_2O_3 has a columnar structure. Er_2O_3 layer formed on each buffer layer had finer structure without buffer layer. It has been also detected that each element does not exist so much in each layer by diffusion during fabrication according to STEM-EDS and HAADF imaging. [doi:10.2320/matertrans.M2016313]

(Received September 5, 2016; Accepted November 28, 2016; Published January 16, 2017)

Keywords: *erbium oxide, buffer layers, metal organic chemical vapor deposition (MOCVD), microstructure, transmission electron microscopy*

1. Introduction

Er_2O_3 has been focused on a material as an insulating coating for a liquid lithium blanket.[1)] In the practical usage point of view, hydrogen permeation test for the advanced breeding blanket system is important using the ideal samples which have coated surface by Er_2O_3. Hishinuma *et. al.* succeeded to form Er_2O_3 film on SUS316 by MO-CVD method by their original way, and it shows lower roughness of film surface and nice property for scratch test,[2)] and its film has been investigated in our previous report.[3)]

In order to enhance the performance of Er_2O_3 coating as an electrical insulator and e hydrogen permeation burrier, it is necessary to form thicker coating is higher crystallinity. However, the epitaxial growth like a chemical vapor deposition is difficult to form thicker coating layer on a metal substrate. For the thicker oxide coating formation, generally, it is effective to stack simply oxide coating into layer by layer. Furthermore, the crystallinity of oxide coating layer is improved by the matching of the lattice constant between the oxide layer and the buffer layer. There is a report for $YBa_2Cu_3O_7$ (YBCO) superconductor which has buffer layers of CeO_2 and Y_2O_3, and YBCO crystalline grow epitaxy on those layers.[4)]

In our recent study, yttrium oxide and cerium oxide, having the similar lattice constant to that of erbium oxide crystalline and a substrate material, and the effect of buffer layer formation on the nano-structure and the hydrogen permeation property of double stacked coating layer was investigated, and its possibility to form these buffer layers on the SUS substrate. Er_2O_3 and Y_2O_3 and CeO_2 crystalline have the cubic structure, and Er_2O_3 and Y_2O_3 are C-rare earth structure, and CeO_2 is CaF_2 structure. The lattice parameters of Er_2O_3 and Y_2O_3 are 1.06 nm, almost similar to each other, and the lattice parameter of CeO_2 is the half of 1.06 nm.[5)]

In this study, microstructures and the relationship between Er_2O_3 layer and buffer-layers of Y_2O_3 or CeO_2 formed by RF-sputtering method on a substrate has been investigated using transmission electron microscopy (TEM) for the cross sectioned TEM samples prepared by the focused ion beam technique to investigate crystallinity and the morphology of their crystalline.

2. Experimental Procedure

The buffer-layers of Y_2O_3 or CeO_2 has been formed by RF-sputtering method on a commercial SUS 316 disc plate, and then the Er_2O_3 film has formed by a metal organic chemical vapor deposition (MOCVD) method. The buffer layers of Y_2O_3 and CeO_2 were fabricated by the conventional RF sputtering method. The condition of MOCVD was the same as the previous report[3)] using metal organic material of $Er(IBPM)_3$ and the substrate temperature was 500°C. The mention of thickness of Er_2O_3 was about 150 nm. The roughness of Er_2O_3 was about 25 nm. After MOCVD, sample discs took out from the machine, and provided for analysis of microstructure or the hydrogen permeation test. Scanning, transmission, and scanning-transmission electron microscopes (SEM (Hitachi S3500), TEM (Topcon EM-002B), STEM (Hitachi HD7200)) were used for analysis of microstructure in samples.

Small tips of cross sectional TEM (X-TEM) samples for TEM observation were prepared perpendicular to the sample surface and parallel to gas flow on MOCVD by FIB method. FIB was Hitachi FB-2100. The dimension of small tip of X-TEM sample was about 12 μm × 2 μm, and its thickness is less than 100 nm. The accelerating voltage of FIB was 40 kV

[*1]Graduate Student, University of Toyama. Present address: Ahresty Corp., Toyohashi 441–3153, Japan
[*2]Corresponding author, E-mail: matsuda@eng.u-toyama.ac.jp

for Ga+ ion, and the aperture size was 520 μm in the first for rough milling, and then changed to the smallest aperture size of 15 μm for final milling, gently.

3. Results and Discussion

3.1 100 nm CeO_2

Figure 1 show overviews and SEM images of sample with Er_2O_3/100 nm CeO_2 –buffer/SUS, Er_2O_3/100 nm Y_2O_3 –buffer/SUS, Er_2O_3/500 nm CeO_2 –buffer/SUS, and Er_2O_3/500 nm Y_2O_3 –buffer/SUS substrates. A rainbow color depending on the difference of thickness by oxide can be seen on the surface of each sample in Fig. 1(a), (c), (e) and (g). White arrows indicate a direction of gas flow on MOCVD process. Figure 1(b), (d), (f) and (h) show SEM image of their surfaces. No remarkable particles can not observed on those surfaces, while small particles have confirmed on the surface in our previous sample without CeO_2 buffer.[3)]

Figure 2 shows TEM images obtained for the X-TEM sample of Er_2O_3/100 nm CeO_2 –buffer/SUS substrate. Figure 2(a) shows a whole area of this sample, and 5 layers can be seen in this picture. An enlarged picture in (a) marked by a white broken square is shown in Fig. 2 (b). These are tungsten deposition, Er_2O_3 layer, CeO_2-buffer, white unknown layer and a SUS substrate. The columnar structure can be confirmed in Er_2O_3 layer, while small grains can be seen in CeO_2-buffer layer. The width of Er_2O_3 column and size of CeO_2 were 74 nm and 33 nm. The roughness of the interface between Er_2O_3 and CeO_2, and of SUS substrate were 33 nm and 30 nm, respectively. A white layer also can be seen between CeO_2-buffer layer and a SUS substrate. It will be some oxide layer on a substrate according to our previous report.[3)] A columnar structure is visible on a dark field image of Fig. 2(c) which has been obtained for an area marked by a white square in Fig. 2(b). The selected area electron diffraction (SAED) patterns were obtained from the regions of Er_2O_3 and CeO_2 buffer layers as shown in Fig. 2(d) and (e), and these incident electron beam directions were indexed as $<121>_{Er2O3}$ and $<121>_{CeO2}$. The chemical analysis has been performed by TEM-EDS for the interface marked by a line of A-A' in Fig. 2(b). The oxygen has been omitted in this analysis because of difficulty for quantitative analysis. In Fig. 3, Er is definitely the highest at the left on side of Er_2O_3 layer and Ce is the highest at the middle region of CeO_2-buffer layer. Fe is predominant at the right on side of SUS 316 substrate, which shows 9–10 mass%Ni and 18–19 mass%Cr close to the standard SUS 316 steel. An inserted figure of the left on side is the position from 135–225 nm, and this shows interesting behavior of Ce, which increased at the boundary inside Er_2O_3 layer. It is suggested that Ce diffused from a buffer into the Er_2O_3 layers during MOCVD process, because of the similarity of crystal structure between CeO_2 and Er_2O_3. The oxide layer around 360 nm of the position, which can be seen a white layer in Fig. 2(a), indicates higher intensity of Fe, Cr and Ni rather than those in the buffer layer. The inserted EDS profile has been obtained for the mid-point of unknown layer, and it includes oxygen as the same as the previous report.[3)] This unknownlayer is probably a natural Cr oxide (Cr_2O_3) on the SUS substrate.

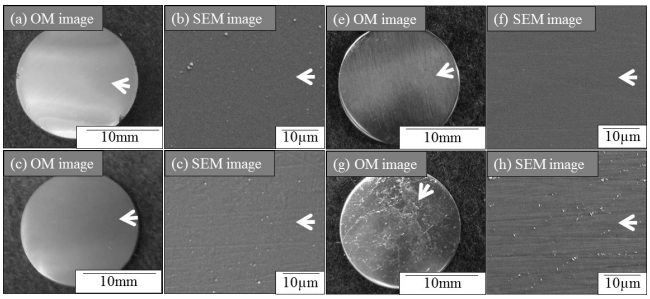

Fig. 1 Overviews and SEM images of samples. (a), (b) Er_2O_3/100 nm CeO_2 –buffer/SUS, (c), (d) Er_2O_3/100 nm Y_2O_3 –buffer/SUS substrates, (e), (f) Er_2O_3/500 nm CeO_2 –buffer/SUS, and (g), (h) Er_2O_3/500 nm Y_2O_3 –buffer/SUS substrates. (a), (c), (e), (g) their outlooks, and (b), (d), (f), (h) SEM images of samples.

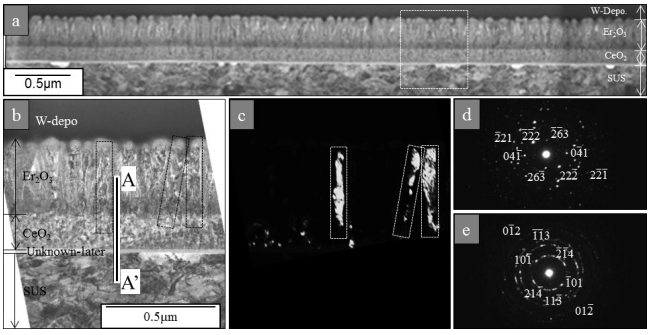

Fig. 2 TEM images obtained for the X-TEM sample of Er_2O_3/100 nm CeO_2 –buffer/SUS substrate. (a) a bright field TEM image of whole area of this sample, (b) and (c) an enlarged picture and a dark field image in (a) marked by a white broken square. (d) and (e) SAED patterns obtained for Er_2O_3 and CeO_2 layers.

Figure 4 shows images obtained by FE-STEM for the same sample of Fig. 2. Figure 4(b) and (c) are enlarged pictures marked by a black square in Fig. 4(a). The CeO_2-buffer consists of small crystalline, and Er_2O_3 layer has columnar structure like as the dendrite in HAADF-STEM image of Fig. 4(c). As there are no any chill crystalline or special gap between Er_2O_3 and CeO_2 buffer, it suggested that Er_2O_3 grows from the CeO_2 buffer by MOCVD method continuously, but its morphology is not uniform because of depending on gas flow. A thin layer between SUS substrate and CeO_2 buffer can be seen as black or white color. It is provably an oxide layer. Figure 5 shows STEM-EDS maps obtained for an area marked by a white square in Fig. 4(a). Er, Ce, O and Fe show homogeneous distribution of these elements in each layer. It is noted that Cr-rich layer in Fig. 5(f) corresponds to the black layer in BF-STEM image of Fig. 5(a), and thin Fe layer in Fig. 5(e) can be seen. Small amount of Cr was detected from the CeO_2 buffer layer. This means that Cr oxide layer exists on the SUS substrate and CeO_2 buffer avoids the diffusion of Cr into the Er_2O_3. Thin Fe layer above SUS substrate in Fig. 5(e) was thinner than that in our previous report what did not have CeO_2 buffer layer. It is suggested that CeO_2-buffer also avoids the diffusion of Fe from the SUS substrate during the processing of MOCVD.

3.2 Effect of Thickness of buffer layer

Figure 6 shows TEM images obtained for X-TEM of Er_2O_3/500 nm CeO_2 buffer/SUS substrate. 500 nm CeO_2

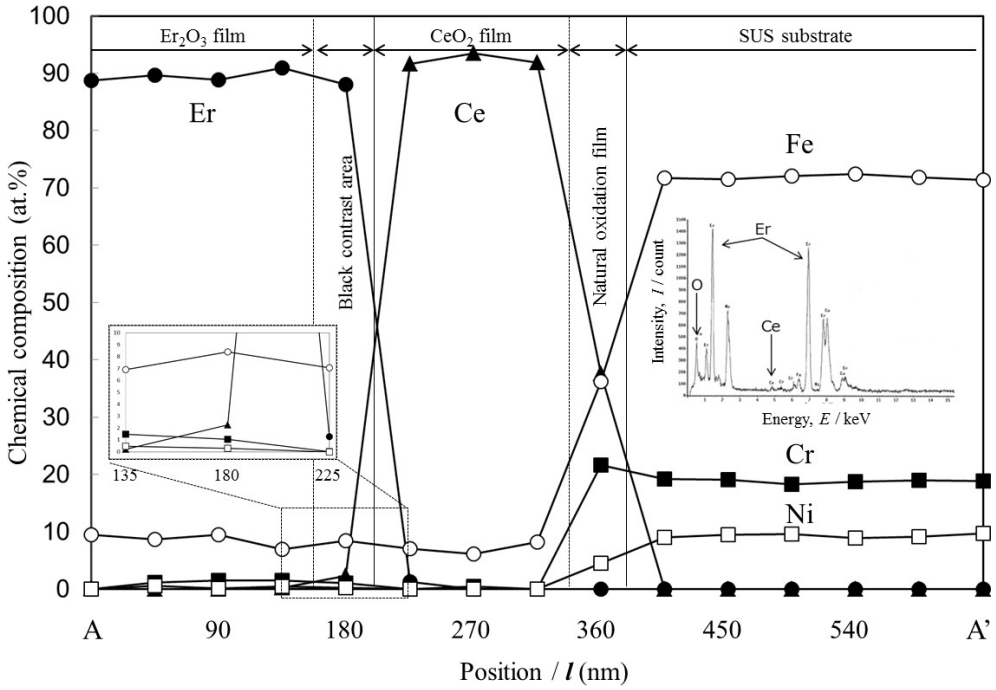

Fig. 3 EDS profiles for Er, Ce, Fe, Cr and Ni elements for line A-A' in Fig. 2 (b). The inserted EDS profile has been obtained for the mid-point of unknown layer.

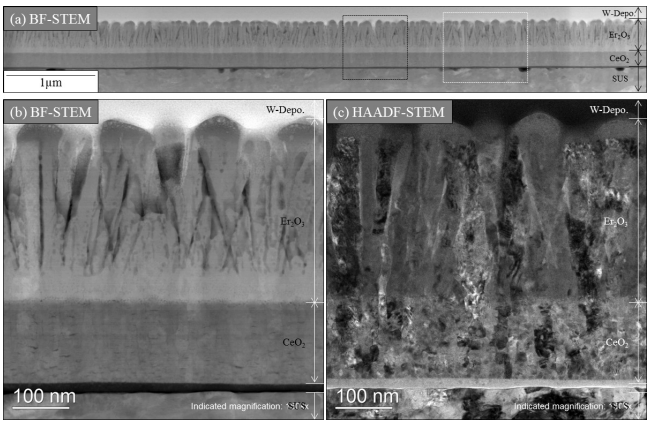

Fig. 4 STEM images obtained for the X-TEM sample of Er_2O_3/100 nm CeO_2 –buffer/SUS substrate in Fig. 2. (a) a BF-STEM image of whole area of this sample, (b) and (c) an enlarged BF-STEM and a HAADF images in (a) marked by a black square.

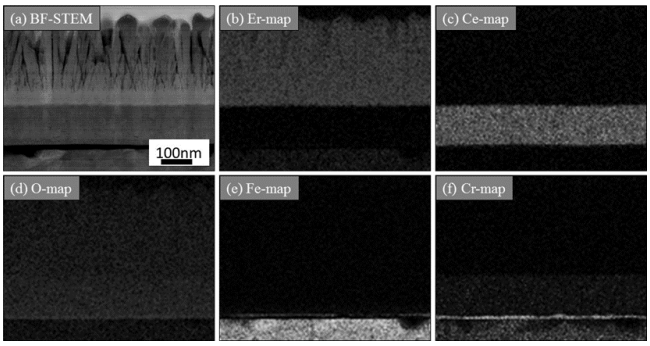

Fig. 5 (a) BF-STEM image and EDS maps of (b) Er, (c) Ce, (d) O, (e) Fe, (f) Cr obtained for the BF-STEM sample of Fig. 2 (a) marked by a white square.

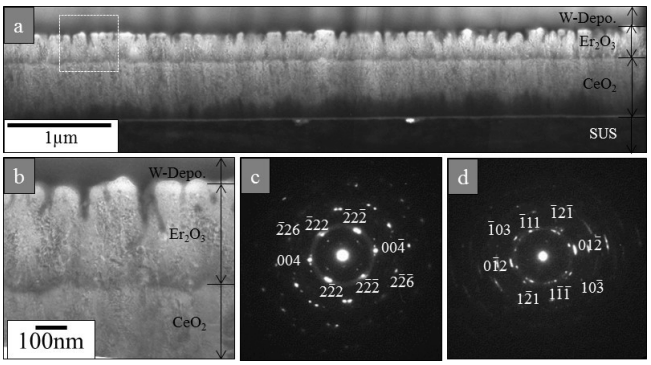

Fig. 6 TEM images obtained for the X-TEM sample of Er_2O_3/500 nm CeO_2 –buffer/SUS substrate. (a) a bright field TEM image of whole area of this sample, (b) an enlarged picture in (a) marked by a white broken square. (c) and (d) SAED patterns obtained for Er_2O_3 and CeO_2 layers.

buffer can be seen between Er_2O_3 and SUS substrate. The column of Er_2O_3 becomes wider than the sample which has the 100 nm CeO_2 buffer of Fig. 2(a). The surface flatness of Er_2O_3 layer also became smooth. The morphology of CeO_2 was an elongated grain rather than 100 nm CeO_2. The SAED patterns were obtained from the regions of Er_2O_3 and CeO_2 buffer layers as shown in Fig. 6(c) and (d), and these incident electron beam directions were indexed as $<110>_{Er2O3}$ and $<321>_{CeO2}$. The width of Er_2O_3 column and size of CeO_2 were 130 nm and 104 nm. The roughness of the interface between Er_2O_3 and CeO_2, and of SUS substrate were 25 nm and 25 nm, respectively. The thick 500 nm CeO_2 buffer causes worth thermal conductivity, and it introduce slow growth of Er_2O_3 columnar direction, then the width of Er_2O_3 column became wider than a sample without buffer.

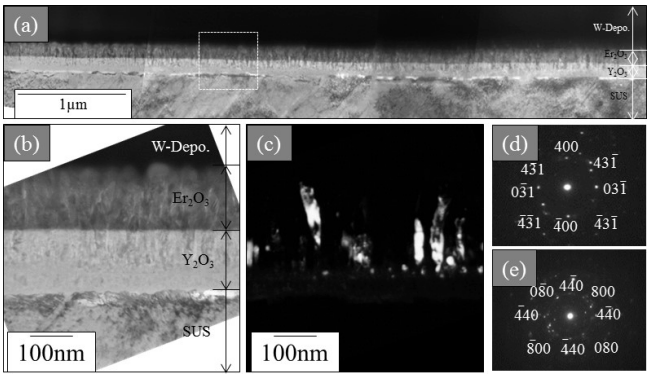

Fig. 7 TEM images obtained for the X-TEM sample of Er_2O_3/100 nm Y_2O_3 –buffer/SUS substrate. (a) a bright field TEM image of whole area of this sample, (b) and (c) an enlarged picture and a dark field image in (a) marked by a white broken square. (d) and (e) SAED patterns obtained for Er_2O_3 and Y_2O_3 layers.

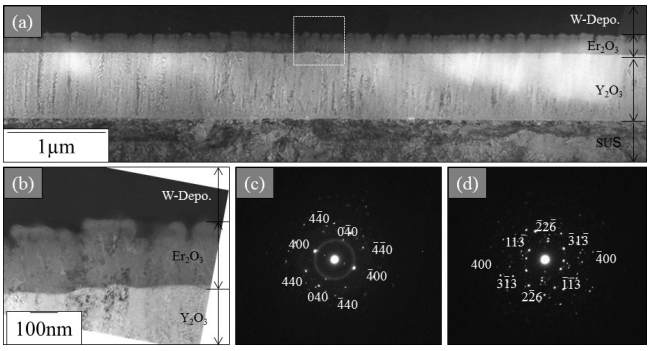

Fig. 8 TEM images obtained for the X-TEM sample of Er_2O_3/500 nm Y_2O_3 –buffer/SUS substrate. (a) a bright field TEM image of whole area of this sample, (b) an enlarged picturee in (a) marked by a white broken square. (c) and (d) SAED patterns obtained for Er_2O_3 and Y_2O_3 layers.

3.3 buffer of Y_2O_3

Figure 7 shows TEM images obtained for X-TEM of Er_2O_3/100 nm Y_2O_3 buffer/SUS substrate. Figure 7(a) shows a whole area of this sample, and 4 layers can be also seen in this picture. These are tungsten deposition, Er_2O_3 layer, Y_2O_3-buffer, and a SUS substrate. The white unknown layer could not be confirmed in this case. The columnar structure can be confirmed in Er_2O_3 and Y_2O_3 buffer layers, while small grains can be seen in CeO_2-buffer layer. According to the analysis of SAED patterns of Fig. 7(d) and (e), $<013>_{Er2O3}$ and $<001>_{Y2O3}$ were indexed. The width of Er_2O_3 column and Y_2O_3 were 60 nm and 17 nm. The roughness of the interface between Er_2O_3 and Y_2O_3, and of SUS substrate were 12 nm and 21 nm, respectively.

Figure 8 TEM images obtained for X-TEM of Er_2O_3/500 nm Y_2O_3 buffer/SUS substrate. The columnar structure of Y_2O_3 buffer and Er_2O_3 can be seen remarkably. The SAED patterns were obtained from the regions of Er_2O_3 and Y_2O_3 buffer layers as shown in Fig. 8(c) and (d), and these incident electron beam directions were indexed as $<001>_{Er2O3}$ and $<031>_{Y2O3}$. As Er_2O_3 and Y_2O_3 have the same crystal structure of C-rare earth structure, this is an equivalent relationship with Fig. 7(d) and (e). The width of Er_2O_3 column and Y_2O_3 were 120 nm and 60 nm. The roughness of the interface between Er_2O_3 and Y_2O_3, and of SUS substrate were 20 nm and 17 nm, respectively.

In our recent report for the single layer of Er_2O_3 on the SUS substrate[3], crystalline of Er_2O_3 were nucleated at some sites on the substrate surface, for example natural oxide layer, those nucleus preferentially grow from those nucleation site, and then coarse crystalline were formed on the substrate. The column width of Er_2O_3 on SUS substrate was 260 nm. On the other hand, if there is a buffer layer of CeO_2 between Er_2O_3 and SUS substrate, the nucleation of Er_2O_3 depends on the roughness of 25–30 nm for CeO_2. The column width of Er_2O_3 on CeO_2/SUS was 70 or 130 nm for the thickness of 100 or 500 nm of CeO_2, and that column width was 1/3 or a half of Er_2O_3 on SUS without buffer. A buffer layer of Y_2O_3 was also shown the similar behavior to the CeO_2 layer. The roughness of Y_2O_3 was 12–20 nm, and the column width of Er_2O_3 on Y_2O_3/SUS was 60 or 120 nm for the thickness of 100 or 500 nm of Y_2O_3. This result has suggested that the surface roughness is important factor to nucleate and control the column thickness of Er_2O_3.

The column width of columnar shaped Y_2O_3 was 17 or 60 nm, and it is smaller than 33 or 104 nm of granular shaped CeO_2, even thickness is different from 100 to 500 nm. As Er_2O_3 nucleates and grows on or at those crystalline of CeO_2 or Y_2O_3, the column width of Er_2O_3 is controlled by the size of crystalline of buffer layers. In this study, the crystallographic orientation relationship can not be confirmed between CeO_2 and Er_2O_3, or Y_2O_3 and Er_2O_3. As Y_2O_3 and Er_2O_3 have the same crystal structure and similar lattice parameter of 1.0602 nm and 1.0548 nm to each other.[6] Its misfit was calculated by the previous work[5], and those were about 0.51% between $\{001\}_{Y2O3}$ and $\{001\}_{Er2O3}$ of the cube-cube relationship. Y_2O_3 and Er_2O_3, however, has been shown <001> and <031> orientation relationship in Figs. 7 and 8. This is rotating relationship about 18 degrees to each other, its misfit is calculated using other eq. (1) as follows;

$$misfit^{(hkl)Er2O3}_{(hkl)Y2O3}[\%] = \left|\frac{d(hkl)_{Er2O3} - d(hkl)_{Y2O3}}{d(hkl)_{Er2O3}}\right| \times 100 \qquad (1)$$

The lattice misfit was calculated as 9.7% between $\{007\}_{Er2O3}$ and $\{71\bar{3}\}_{Y2O3}$, or 5.2% between $\{007\}_{Er2O3}$ and $\{226\}_{Y2O3}$. As these misfit values are not small, the growth of Er_2O_3 on Y_2O_3 probably depends on the similarity of crystal structure. The orientation relationship between Er_2O_3 and Y_2O_3 or CeO_2 probably depends on the condition during MOCVD process, although the column width of Er_2O_3 is controlled by crystalline size on the surface of Y_2O_3 or CeO_2 buffer according to the present result.

4. Conclusions

(1) CeO_2 or Y_2O_3 buffer layer of 100 or 500 nm in thickness has been prepared on the SUS 316 substrate by RF-sputtering method, and the Er_2O_3 layer could be formed on CeO_2 or Y_2O_3buffer layers about 150–280 nm.

(2) The surface roughness of Er_2O_3/CeO_2/SUS and Er_2O_3/Y_2O_3/SUS were 25–30 nm and 12–20 nm respectively, while it was 140 nm without buffer.

(3) CeO_2 with granular structure has been formed on SUS substrate, and it makes smaller columns of Er_2O_3 than the

Er_2O_3 column without CeO_2 buffer. CeO_2 crystalline was depends on thickness of CeO_2 buffer layer.

(4) Y_2O_3 with columnar structure has been formed on SUS substrate, and it makes smaller columns of Er_2O_3 than the Er_2O_3 column without buffer and with CeO_2 buffer. The width of Y_2O_3 column was also depends on thickness of Y_2O_3 buffer layer.

Acknowledgements

A part of this project has been supported by NIFS research foundation 2015, and President description, University of Toyama (2015).

REFERENCES

1) B.A. Pint, P.F. Tortorelli, A. Jankowski, J. Hayes, T. Muroga, A. Suzuki and O.I. Yeliseyeva: J. Nucl. Mater. **329–333** (2004) 119–124.
2) Y. Hishinuma, S. Murakami, K. Matsuda, T. Tanaka, Y. Tasaki, T. Nagasaka, A. Sagawa and T. Muroga: Plasma & Fusion Research **7** (2012) 2405127-1–2405127-4.
3) T. Shikawa, K. Matsuda, Y. Hishinuma, K. Nishimura, T. Tanaka, T. Muroga and T. Sato: Mater. Trans. **55** (2014) 1781–1785.
4) H. Zhang, J. Yang, H. Liu and S. Wang: Physica C **470** (2010) 1998–2001.
5) Y. Hishinuma, T. Tanaka, T. Shinkawa, S. Murakami, K. Matsuda, T. Watanabe, T. Nagasaka, A. Sagara and T. Muroga: Fusion Sci. Tech. (Paris) **66** (2014) 221–227.
6) JCPDS (Y_2O_3)00-005-0574, (Er_2O_3)00-008-0050, (CeO_2)34-0394.